THE BEHAVIOUR OF SHORT WAVES IN THE PRESENCE OF LARGE LONG WAVES

R.C.T.Rainey, Rod Rainey & Associates, Bath BA1 5SU, U.K. *enquiries@RRandA.co.uk* and Sustainable Energy Research Group, University of Southampton SO17 1BJ, U.K. *r.rainey@soton.ac.uk*

Abstract
Some offshore structures have a resonant response to short waves, which needs to be considered in combination with the main response to large survival waves. The behaviour of short waves in the presence of large long waves is however a longstanding problem area in marine hydrodynamics. Stokes' expansion diverges and the empirical approximations such as "Wheeler stretching" have no theoretical foundation. This paper explores the problem with a fully-nonlinear numerical simulation, not of the usual boundary-element type, but with a simple numerical scheme based on Fourier series, which is implemented in MATHCAD. It is found that the second-order difference frequency wave, from Stokes' expansion, is rapidly joined by other waves of intermediate wavelengths, travelling with various velocities. The behaviour is complicated, but does not appear to be chaotic.

Background – practical importance of the issue, and its theoretical difficulty
Traditionally, fixed offshore structures are designed so that their natural periods are sufficiently short (< 3s) that there is no dynamic response to the waves. Some recent structures, however, have natural periods sufficiently long (> 4s) that their dynamic response to waves is noticeable, and contributes to the 100-year extreme structural response. Calculating this extreme response is then a matter of combining the effect of large survival waves of long period (> 12s), with the effect of much shorter waves at the natural period.

Here a well-known difficulty arises. If the long and short waves are simply superimposed according to the linear theory, the short wave "blows up" on the crest of the long one, because of its strong exponential depth dependence. A 3:1 ratio of wave period corresponds to a 9:1 ratio of wavelength, so if the exponential magnification of the long wave in its crest is 1.3, say, which is typical, then it is $1.3^9 = 10.6$ in the short wave in the same crest. This is clearly physically implausible, and from a theoretical point of view means that the linearity assumption has broken down – when we calculate the second-order wave components (see below) they are larger than the first-order, so Stokes' expansion is diverging.

The traditional engineering assumption ("Wheeler stretching" [1]) is that the short wave is the same as it would be on its own in otherwise-still water, and is simply transported up to the crest of the long wave. This is however almost certainly a non-conservative assumption, because at sea all large waves are observed to have foam on their crests ("white horses") which could be local breaking of shorter waves. Also, if the bandwidth of the waves is restricted to 2:1 period ratio, linear theory is observed in the laboratory [2] to give a good model of the wave kinematics, without any "Wheeler stretching".

This paper explores the behaviour of a short wave in the presence of large long wave of 10 times the wavelength (i.e. period ratio of $\sqrt{10} = 3.16$:1), by fully-nonlinear numerical simulation. To avoid the complexities of local wave breaking, the steepness of short wave (but not the long wave) is made small.

Numerical method
A method for fully-nonlinear numerical simulation of water waves was first developed in 1976, by Longuet-Higgins and Cokelet [3]. This boundary-element method has since been developed by several workers, e.g. [4], [5]. The late Prof. Peregrine's program was successfully used by the author ten years ago, with his support, on a similar problem [6]. However, no supported version of these boundary-element codes is currently commercially available, to the author's knowledge.

This paper accordingly develops a new method, suitable for the present problem where the wave does not break, and our interest is in its frequency content. The fluid domain is periodic of length L, as with the boundary-element method, allowing us to expand the velocity potential ϕ as an N-term Fourier series:

$$\phi = \sum_{n=0}^{N} Re\left(\Phi_n(t) e^{k_n(z+ix)}\right)$$

which inherently satisfies Laplace's equation. Here $k_n = 2\pi n/L$ are the wavenumbers of the Fourier components whose complex amplitudes $\Phi_n(t)$ are arbitrary functions of time, so that they can have any speed. The numerical method has been implemented in MATHCAD for maximum readability; the MATHCAD routine stores $\Phi_n(t_j)$, $d/dt\{\Phi_n(t_j)\}$ and $d^2/dt^2\{\Phi_n(t_j)\}$ at the jth timetep as the N-vectors Φ_j , $D\Phi_j$ and $DD\Phi_j$, respectively. The free surface elevation η is also described as an N-term Fourier series, which (since η is purely real) gives by FFT the elevation η and its slope $\partial\eta/\partial x$ at $2N$ points equally-spaced over L. Their values at the jth timestep are stored in the routine

as the *2N*-vectors ψ_j and $S\psi_j$ respectively. The routine calculates the values of all these vectors at the $(j+1)$th timestep as follows:

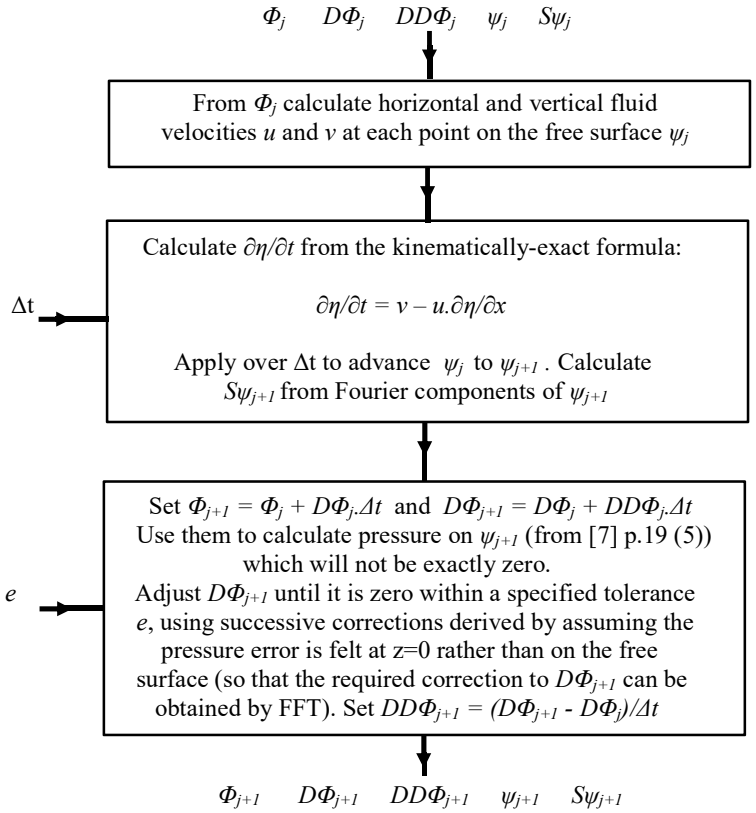

Figure 1. Numerical scheme

Initial runs showed that the scheme was susceptible to a high-frequency "zig-zag" instability, just like the instability seen in boundary element computations [4], [5]. There it is removed by introducing some smoothing of the free surface, the same effect is achieved here by setting the Fourier components Φ of the potential (but not those of the surface elevation η) to zero above some cut-off wavenumber, above which the waves were apparently all numerical instabilities, in that their amplitude was controlled by the computation parameters Δt and e.

Parameters chosen for computation

Length of computational domain	256 m
Length of long wave	256 m (i.e. $k = 2\pi/256 = 0.0245$ m^{-1}, 12.8 s linear-theory period)
Nominal amplitude of long wave	5 m (i.e. 10 m nominal height)
Length of short wave	25.6 m (i.e. $k = 2\pi/25.6 = 0.245$ m^{-1}, 4.05 s linear-theory period)
Nominal amplitude of short wave	5 cm (i.e. 10 cm nominal height)
Number of computational points	256 (i.e. 1 m spacing)
Number of wavenumbers	128 (i.e. $2\pi/256 = 0.0245$ m^{-1} spacing)
Cut-off wavenumber	20 times lowest
Timestep Δt	0.5 milliseconds
Pressure tolerance e on free surface	1 mm head (i.e. 0.01 kPa)

Results

Simulations were started using the velocity potential from 2nd order wave theory, which features a 2nd order potential at the difference-wavnumber, see e.g. [6] eqn. 4.2. The simulation was started from the zero-pressure surface, automatically including all the 2nd order components of surface elevation. As an additional refinement, the 3rd order correction ([7] p.417 (6)) to the speed of the long wave was included in these initial conditions. Results of a 100s run are shown in Figure 2 below.

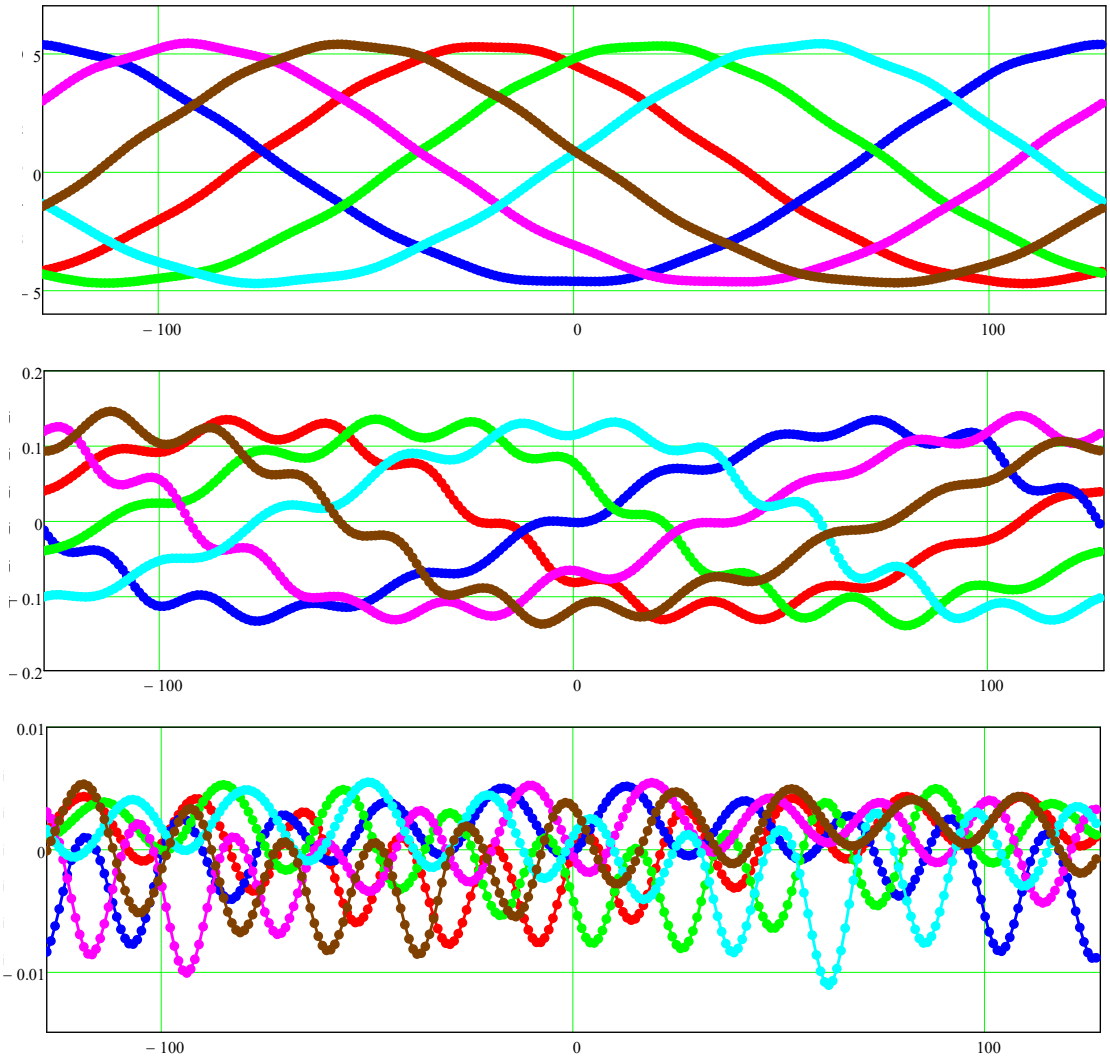

Figure 2. Snapshots over computational domain of surface elevation η (m, top) slope $d\eta/dx$ (m/m middle) & curvature $d^2\eta/dx^2$ (m^{-1}, bottom), after 0s (●●●), 20s (●●●), 40s (●●●), 60s (●●●), 80s (●●●), & 100s (●●●)

The initial shape of the wave shows much less variation in the height of the short wave, between the crest and trough of the long wave, than suggested by linear theory, according to which the amplitude of the short wave should vary by a factor $e^{0.245\times10} = 11.6$. This shows the importance of the 2nd order potential at the difference-wavenumber, which is in phase with the linear short-wave potential in the long-wave trough, and in anti-phase in the long-wave crest. The later development of the short wave largely preserves this feature. However, many other Fourier components are seen in the surface elevation, as may be seen in Figure 3 below.

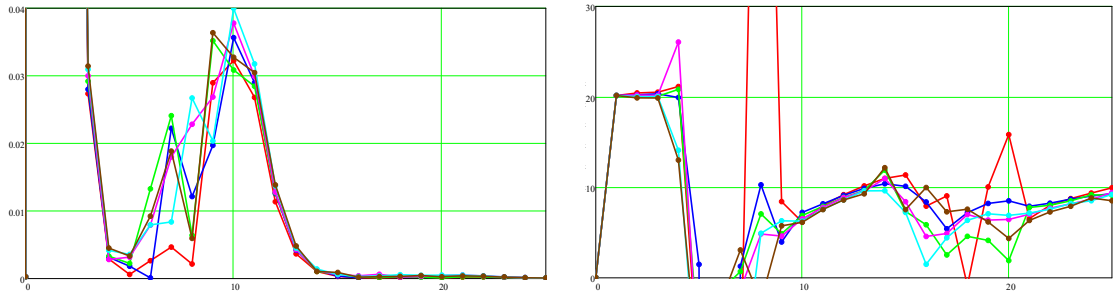

Figure 3. Amplitude (m, left) and speed (ms^{-1}, right) of Fourier components of surface elevation η, as a function of wavenumber (25 components shown, some off-scale). Times shown by colour code of Fig. 2.

The sum and double-wavenumber components are evident, as expected from the well-known 2nd order formulae (e.g. [6] eqn 4.3), but other components are also noticeable, particularly in between the two original wavenumbers. The speeds of the components are also given in Figure 3, and largely follow the 2nd order formulae for the relevant wavenumbers – but again other components, of different speeds, are noticeable, as seen in experiments on focused waves ([6], fig. 4).

More fundamental, and less complicated, are the Fourier components of the potential (it is convenient to consider $D\Phi$ rather than Φ, since $\partial\phi/\partial t$ is directly related to pressure), shown in Figure 4 below.

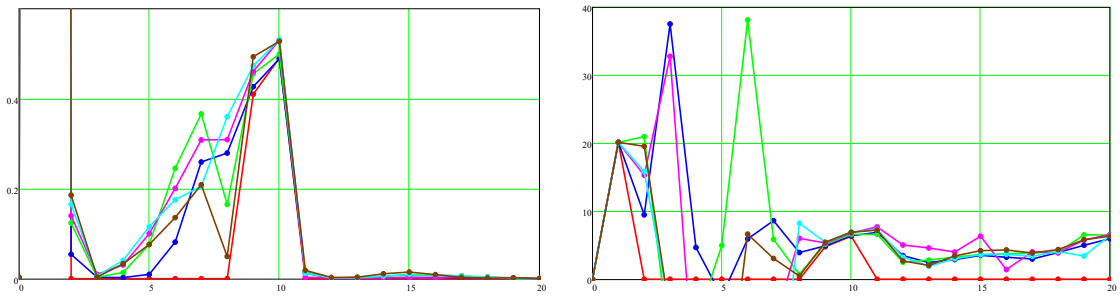

Figure 4. Amplitude (m^2s^{-2}, left) and speed (ms^{-1}, right) of Fourier components $D\Phi$, as a function of wavenumber (first 20 components shown, 1st off-scale). Times shown by colour code of Fig. 2.

Particularly interesting is the variation over time of the component amplitudes, shown in Figure 5 below. This is very complicated (the slight upwards drift reduces with Δt), but does not appear to be chaotic – it is unchanged if a trough, rather than a crest, of the short wave is initially aligned with the crest of the long wave.

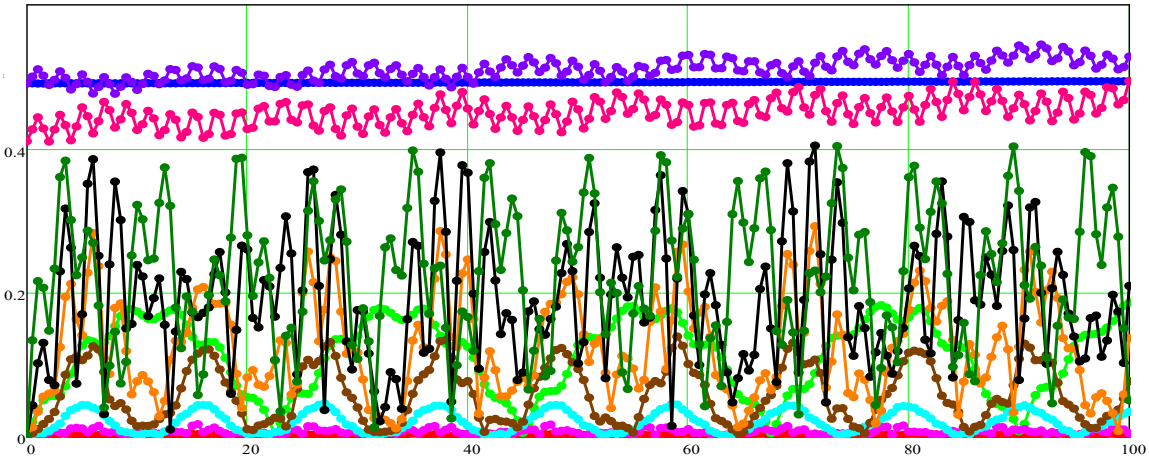

Figure 5. Variation of amplitudes of first 10 Fourier components in $D\Phi$, over 100s.
= 0th, =1st(×0.01), = 2nd, = 3rd, =4th, =5th, =6th, =7th, =8th, =9th, =10th

References

[1] Wheeler, J.D.E. Method for calculating forces produced by irregular waves. *Journal of Petroleum Tech.*, 249 (1970) pp 359-367.

[2] Chaplin, J.R. & Rainey, R.C.T. Long-duration experiments in irregular waves, to determine 10,000-year wave loads on a 3.5m diameter vertical cylinder, *27th IWWWFB*, Copenhagen (2012).

[3] Longuet-Higgins, M.S. & Cokelet, E.D. The deformation of steep surface waves on water. I. A numerical method of computation. *Proc. R. Soc. Lond.* A358 (1976) 1-26.

[4] Dold, J.W. and Peregrine, D.H. An efficient boundary-integral method for steep unsteady water waves. Numer. Meth. for Fluid Dynamics II (Eds. Morton, K.W. & Baines, M.J.), Oxford University Press (1986) pp 671-679.

[5] Dold, J.W. An efficient surface-integral algorithm applied to unsteady gravity waves. *J. Computational Physics*.103 no.1 (1992), pp 90-115.

[6] Rainey, R.C.T. Weak or strong nonlinearity: the vital issue, *J. Eng Maths*, 58 (2007) pp 229-249

[7] Lamb, H. Hydrodynamics. 6th Ed. Cambridge University Press (1932).